*Articles*

# Spectroscopic Characterization of the Photocycle Intermediates of Photoactive Yellow Protein†

Yasushi Imamoto,*,‡ Ken'ichi Mihara,‡ Fumio Tokunaga,§ and Mikio Kataoka‡

*Graduate School of Materials Science, Nara Institute of Science and Technology, Ikoma, Nara 630-0101, Japan, and Department of Earth and Space Science, Graduate School of Science, Osaka University, Toyonaka, Osaka 560-0043, Japan*

*Received March 7, 2001; Revised Manuscript Received July 10, 2001*

ABSTRACT: The absorption spectra of photocycle intermediates of photoactive yellow protein mutants were compared with those of the corresponding intermediates of wild type to probe which amino acid residues interact with the chromophore in the intermediate states. B and H intermediates were produced by irradiation and trapped at 80 K, and L intermediates at 193 K. The absorption spectra of these intermediates produced from R52Q were identical to those from wild type, whereas those from E46Q and T50V were 7−15 nm red-shifted as those in the dark states. The absorption spectra of M intermediates were measured by flash photolysis at room temperature. Those of Y42F, T50V, and R52Q were identical to that of wild type, whereas that of E46Q was 11 nm red-shifted. Assuming that the intermediates of mutants have a structure comparable to that of wild type, these findings suggest the following: Glu46 interacts with the chromophore throughout the photocycle, interaction between the chromophore and Thr50 as well as Tyr42 is lost upon the formation of M intermediate, and Arg52 never interacts with the chromophore directly. The hydrogen-bonding network around the phenolic oxygen of the chromophore would be thus maintained until L intermediate decays, and the global conformational change would take place by the loss of the hydrogen bond between the chromophore and Tyr42. This model conflicts with some of the results of previous crystallographic studies, suggesting that the reaction mechanism in the crystal may be different from that in solution.

Photoactive yellow protein (PYP)[1] (*1*), a putative photoreceptor protein for the negative phototaxis of purple phototrophic bacteria (*2*), is a relatively small (14 kDa) water-soluble protein. Due to this advantage, X-ray crystallography (*3*, *4*) and NMR (*5*) have been applied to the structural analysis of PYP. PYP from *Ectothiorhodospira halophila* is composed of 125 amino acids (*6*) and a chromophore, *p*-coumaric acid binding to the cysteine residue by a thioester bond (*3*, *7*, *8*). The phenolic oxygen of the chromophore (O4) is deprotonated and forms hydrogen bonds with the hydroxy groups of Tyr42 and Glu46, and a hydroxy group of Thr50 forms a hydrogen bond with Tyr42 (*4*). These three residues regulate the absorption maximum of PYP (*9*−*11*). Arg52 exists near the chromophore and stabilizes the hydrogen-bonding network. On photon absorption, a *trans*-*p*-coumaroyl chromophore is isomerized to the cis form (*12*−*16*). Afterward, a proton is transferred from Glu46 to the chromophore (*17*, *18*), and a global conformational change of the protein moiety takes place (*19*−*22*). The photocycle intermediates have been identified by UV−visible spectroscopy using transient measurements at room temperature (*23*−*27*) and steady-state measurements at low temperature (*28*, *29*). On the basis of these results, the structures of photocycle intermediates have been analyzed by X-ray crystallography and a model for the structural change has been proposed (*13*−*15*). PYP is now thought to be the most suitable target to understand the light-capturing mechanism of a photoreceptor protein at the atomic level.

The intermediate of PYP, the structure of which was first proposed, is I2 (also called pB) (*13*). This intermediate has an absorption band in the near-UV region because Glu46 donates a proton to the chromophore (*17*, *18*). The lifetime is ∼100 ms at room temperature. The corresponding intermediate is trapped at −40 °C and is called $PYP_M$ (*18*). On analogy to the meta intermediates of retinal proteins, it is thought to be a physiologically important intermediate. Its structure was analyzed by time-resolved crystallography on a millisecond time scale. The resulting model shows that the phenol part of the chromophore rotates on photoisomerization. As a result, the hydrogen-bonding network among

† This work was supported in part by a Grant-in-Aid for Scientific Research from the Ministry of Education, Culture, Sports, Science, and Technology of Japan, by Kansai Research Foundation for Technology Promotion, and by a SUNBOR GRANT.

* Correspondence should be addressed to this author. Tel: 81 743 72 6101. Fax: 81 743 72 6109. E-mail: imamoto@ms.aist-nara.ac.jp.

‡ Nara Institute of Science and Technology.

§ Osaka University.

[1] Abbreviations: PYP, photoactive yellow protein from *Ectothiorhodospira halophila*; Tris, tris(hydroxymethyl)aminomethane; MOPS; 3-(*N*-morpholino)propanesulfonic acid; FTIR, Fourier transform infrared.

10.1021/bi010468u CCC: $20.00 
Published on Web 11/06/2001

the chromophore, Tyr42 and Glu46, is broken and a new hydrogen bond is formed between the chromophore and Arg52.

The structure of pR (also called I1), a precursor of I2, was later proposed by time-resolved crystallography on a nanosecond time scale (*14*). pR is a red-shifted intermediate observed on a nanosecond−microsecond time scale (*23*, *24*). The intermediate corresponding to pR is trapped at −80°C and is called $PYP_L$ (*29*). Structural modeling reveals that the phenol part rotates for formation of pR. As a result, while the movement of the phenol ring is small, the O4 of the chromophore is removed from Glu46, and the hydrogen bond is broken.

The early intermediate of PYP has been trapped at −124 °C and the structure analyzed (*15*). Irradiation condition suggests that this intermediate is $PYP_{BL}$, the blue-shifted intermediate which appears between $PYP_L$ and the primary intermediate trapped at liquid-nitrogen temperature ($PYP_B$) (*29*). In this model, the thioester part is flipped upon isomerization, and the hydrogen-bonding network around O4 of the chromophore is maintained in $PYP_{BL}$.

If PYP chromophore sequentially assumes such structures as proposed by crystallography, the thioester part first flips for isomerization (PYP → $PYP_{BL}$), and then the whole of the chromophore rotates ($PYP_{BL}$ → $PYP_L$). Subsequently, the phenol part of the chromophore relaxes to form a hydrogen bond with Arg52 ($PYP_L$ → $PYP_M$), and finally PYP is recovered by flipping the phenol part for reisomerization ($PYP_M$ → PYP). This reaction scheme shows a large movement of the chromophore. In the case of rhodopsin, one of the most efficient photoreceptor proteins, it is considered that the $\beta$-ionone ring region of an *11-cis*-retinal chromophore is fixed, and the Schiff base linkage part rotates to minimize the movement (*30*, *31*). While the chemical structure of retinal is completely different from that of *p*-coumaric acid, the primary photochemical event in both systems is the isomerization of the chromophore. Therefore, the movement of PYP chromophore during the photocycle is possibly small. In fact, recent FTIR studies suggested that the hydrogen bond between chromophore and Glu46 is conserved in $PYP_L$ (*16*, *32*, *33*). The difference in the experimental condition (low temperature or room temperature, excitation energy, crystal condition) might cause the difference in the reaction pathway.

Because the possibility that the reaction in the crystal is different from those in other conditions cannot be excluded, spectroscopic evidences which provides structural information must be sufficiently obtained. Moreover, such comparative investigation would reveal the essence of the photoreaction mechanism. In the present study, to analyze the interaction between chromophore of PYP and nearby amino acid(s), site-directed mutagenesis was applied (*9*−*11*, *34*). We previously prepared several PYP mutants in which an amino acid residue near the chromophore is replaced (*9*). The absorption maximum of R52Q (446 nm) was similar to that of wild type (446 nm), whereas those of Y42F, E46Q, and T50V are red-shifted (458, 460 and 457 nm, respectively). This indicates that Tyr42, Glu46, and Thr50 are proximate to the chromophore and involved in the spectral tuning, but direct interaction between the chromophore and Arg52 is not present (*9*, *10*). Point mutation thus provides clear information about the environment of the chromophore. For the intermediate, the same analysis should be possible: the mutation at the amino acid residue which interacts with the chromophore in the intermediate would shift the absorption spectrum of the intermediate. For this purpose, mutations at Tyr42, Glu46, and Arg52 would be suitable since it is proposed that O4 of the chromophore forms hydrogen bonds with Tyr42 and Glu46 in the dark state and $PYP_{BL}$ and with Arg52 in $PYP_M$. However, a mutant which lacks Tyr42 is much less stable than the wild type: Y42F and Y42A are in equilibrium between yellow form and colorless form even at neutral pH (*9*, *11*, *35*). The coexistence of the colorless form prevents the precise measurement of the absorption spectra of the intermediates in the steady-state measurements at low temperature. Therefore, a mutation at Thr50 has been noted, which forms a hydrogen bond with Tyr42. Although Thr50 interacts with the chromophore indirectly, it is involved in color tuning as shown by the red-shift of T50V and T50A (*9*, *11*). In this study, the absorption spectra of the intermediates of wild type, E46Q, T50V, and R52Q were compared with each other and the interactions between the chromophore and nearby amino acid(s) investigated.

## MATERIALS AND METHODS

*Sample Preparation.* Wild-type PYP of *E. halophila* and its mutants, E46Q, T50V, and R52Q, were produced using a heterologous overexpression system by *Escherichia coli* and purified by ammonium sulfate precipitation and DEAE-Sepharose CL6B (Amersham Pharmacia Biotech) column chromatography as reported previously (*9*). For low-temperature measurements, PYP was suspended in Tris buffer (10 mM Tris-HCl, 150 mM NaCl, pH 8.1) and mixed with 2 volumes of glycerol to lower the turbidity on freezing. For measurements at ambient temperature (∼25 °C), PYP was suspended in MOPS buffer (10 mM MOPS, 150 mM NaCl, pH 7.0).

*Low-Temperature UV−Visible Spectroscopy.* Low-temperature UV−visible spectroscopy was carried out using a Shimadzu (Kyoto, Japan) UV-2400PC spectrophotometer equipped with an optical cryostat (Optistat DN, Oxford). Temperature was controlled by an Oxford ITC502 (*18*). A silicon rubber spacer (6 mm inner diameter and 2 mm thickness) was sandwiched between a quartz window and an opal glass (Sigma-Koki, Saitama, Japan), which was used as a sample cell. Reference beam of the spectrophotometer was also diffused by another opal glass. Opal glasses compensated the light scattering caused by the crack of the sample at 80 K. A 1 kW slide projector (Rikagaku, Tokyo, Japan) was used as an irradiation light source. Blue light (436 nm) and green light (500 nm) were obtained using optical interference filters (BJ43161 and BJ43169, Edmund Scientific), and yellow light (>450 nm) was with a glass cutoff filter (Y47, Asahi Techno Glass, Tokyo, Japan). The irradiation light was passed through a 4-cm water layer to remove heat radiation. A removable mirror at an angle of 45° was placed on the path of the monitoring beam of spectrophotometer to lead the irradiation light.

*Flash Photolysis at Ambient Temperature.* The transient difference absorption spectra on a millisecond time scale were measured by a multichannel CCD/fiber optic spectroscopy system (S2000 system, Ocean Optics). The deuterium lamp of a Beckman DU650 spectrophotometer was used as

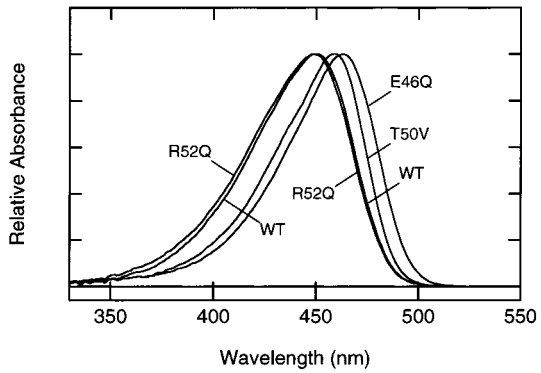


FIGURE 1: Absorption spectra of wild-type PYP, E46Q, T50V, and R52Q in 66% glycerol buffer at 20 °C.

a monitoring light source. The integration time was set at 4 ms, and spectral data were stored every 20 or 170 ms. The first spectrum (dark state) was used as a baseline, and just before the measurements of the second spectrum, PYP was excited by a short arc xenon flash lamp (SA200, Eagle, Kawasaki, Japan) which was triggered by a delay pulse generator (DG535, Stanford Research Systems). A glass cutoff filter (Y43, Asahi Techno Glass, Japan) was used to obtain a yellow flash (>410 nm), which was guided to the top of the quartz sample cell (1 cm × 1 cm) by an optical fiber. The absorbance of the sample at the absorption maximum was about 0.6 in 1 cm light path length. The data presented here are the averages of 64 measurements.

## RESULTS AND DISCUSSION

*Spectral Analysis of Primary Intermediates at Low Temperature.* The absorption maxima of wild type, E46Q, T50V, and R52Q are 446, 460, 457, and 446 nm, respectively (*9*). They are 1−4 nm red-shifted in 66% glycerol buffer (450, 463, 458, and 448 nm, respectively, at 20 °C) (Figure 1). To study the changes in the chromophore/protein interaction during the photocycle, the spectral shapes of the intermediates were analyzed by low-temperature UV−visible spectroscopy (*29*) (Figure 2). Our preliminary experiments on mutants demonstrated that the intermediates corresponding to $PYP_B$, $PYP_H$, and $PYP_L$ of wild type are trapped at the same temperatures as for the wild type (data not shown). The spectra for E46Q measured at low temperature were in good agreement with those measured at room temperature (*10*, *36*). These facts made it possible to compare the spectral shapes of intermediates produced from mutants simply and unambiguously.

The samples used for the spectral analyses of $PYP_B$, $PYP_H$, and $PYP_L$ contained 66% glycerol. It has been reported that glycerol has large effects on the kinetics of the formation and decay of $PYP_M$ as a consequence of its viscosity (*37*), which may also affect the nature of the protein conformational change occurring on the other conversion steps. However, the recent FTIR studies at room temperature demonstrated that no remarkable protein conformational change takes place in PYP → $PYP_L$ conversion (*32*, *33*). The structural changes for formation of these intermediates are thus considered to be localized to the chromophore and nearby amino acids even at room temperature. In fact, the difference absorption spectrum between PYP and $PYP_L$ measured at 193 K using 66% glycerol sample (*29*) is identical to that obtained by transient spectroscopy on a

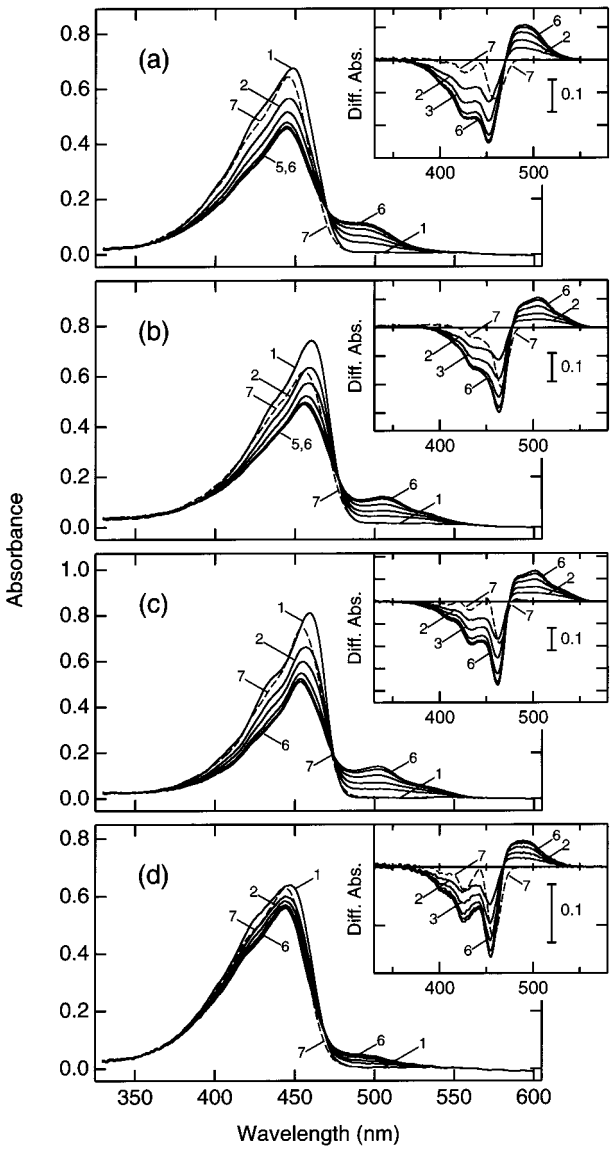


FIGURE 2: Photoreaction of PYP and mutants at 80 K. Wild-type PYP (a), E46Q (b), T50V (c), or R52Q (d) in 66% glycerol buffer was cooled to 80 K (curve 1) and irradiated with 436 nm light for a total of 5, 10, 20, 40, and 80 s (curves 2−6, respectively). It was then irradiated with >450 nm light for 2 min, followed by 500 nm light for 1 min (curve 7). Insets: Difference absorption spectra before and after the irradiation were calculated by subtracting curve 1 from curves 2−7 in each data set.

microsecond time scale at room temperature using the sample without glycerol (*23*, *24*). It indicates that at least the chromophore/protein interactions in the frozen sample are identical to those at room temperature before the decay of $PYP_L$. The wild-type PYP/66% glycerol sample was set in the optical cryostat and cooled to 80 K. It was then irradiated with 436 nm light (Figure 2a). By irradiation, the absorbance at 350−470 nm decreased and that at 470−550 nm increased, indicating the formation of the primary intermediate of PYP ($PYP_B$) (*29*). To show the spectral changes more clearly, the difference absorption spectra before and after the irradiation were calculated (Figure 2a, inset). A clear isosbestic point was observed at 470 nm. However, $PYP_H$, a blue-shifted intermediate, was also formed at this temperature (*29*). In fact, $PYP_B$ disappeared following subsequent irradiation with >450 nm light and 500 nm light, but the absorption spectrum (curve 7) was remarkably different from that of PYP (curve

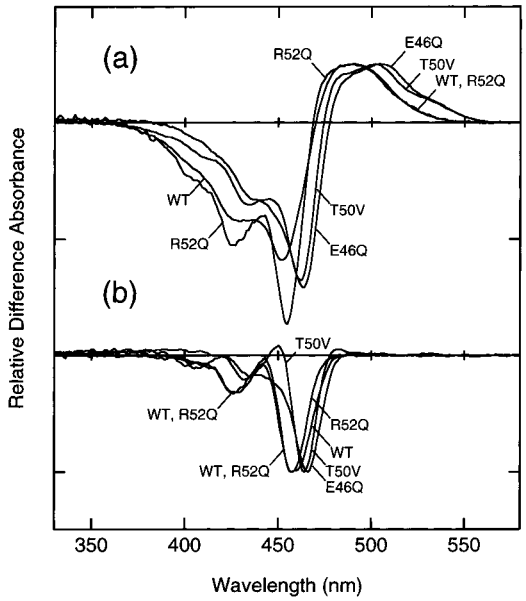


FIGURE 3: Comparison of the absorption spectra of $PYP_B$ (a) and $PYP_H$ (b). Curves 6 and curves 7 in the insets of Figure 2a−d were reproduced after normalization at their difference absorption maxima (a and b, respectively).

1). Because the extinction coefficient of $PYP_H$ is comparable to or lower than that of PYP over the whole visible region (*29*), the difference spectra (curve 7 in inset of Figure 1a) has no positive absorbance region.

The same experiments were performed using E46Q (Figure 2b), T50V (Figure 2c), and R52Q (Figure 2d). Qualitatively similar spectral changes were observed in these mutants upon irradiation with 436 nm light (curves 2−6 in the insets) and 500 nm light (curves 7 in the insets). The former had a broad positive band and characteristic negative band having a prominent fine structures. The latter had negative band with fine structures but no positive absorbance region. These spectral changes indicate the formation of intermediates corresponding to $PYP_B$ and $PYP_H$.

The spectral changes in the mutants observed at 80 K were compared with those of wild-type PYP (Figure 3). In Figure 3a, curves 6 in the insets of Figure 2a−d are reproduced after normalization. These are the mixtures of B and H intermediates *minus* dark states. At 80 K, the regions of wavelength at which the absorbance of dark states are small enough (less than 5% of maximal absorbance) are >477 nm for wild type, >484 nm for E46Q, >479 nm for T50V, and >475 nm for R52Q (Figure 2). Therefore, the difference in the spectral shapes of $PYP_B$, $E46Q_B$, $T50V_B$, and $R52Q_B$ can be examined by comparing the positive bands in these regions. The shape and location of the positive band in R52Q were identical to those of wild type, whereas those in E46Q and T50V were 15 and 12 nm red-shifted, respectively (Figure 3a).

Similarly, curves 7 in the insets of Figure 2a−d are reproduced after normalization to compare the absorption spectra of $PYP_H$, $E46Q_H$, $T50V_H$, and $R52Q_H$ (Figure 3b). The difference spectrum in wild-type PYP was almost identical to that in R52Q. Because the absorption spectra in their dark states are identical, those of $PYP_H$ and $R52Q_H$ are also considered to be identical. Although the difference absorption maximum in E46Q and T50V were 9 and 7 nm red-shifted, respectively, the spectral shape was similar to those in wild type and R52Q: they had two sharp negative bands and only a small positive absorbance region. The similar spectral shape indicates that the absorption maxima and extinction coefficients of $E46Q_H$ and $T50V_H$ relative to those of E46Q and T50V are similar to those in the wild type. In addition, the extinction coefficients of $PYP_H$ are smaller than that of PYP at >413 nm but comparable at <413 nm (*29*). Therefore, if the absorption spectrum of the dark state is red-shifted without a red-shift of H intermediate, the difference spectrum between H intermediate and dark state should have a positive band at around 410 nm unlike the experimental data. The absorption spectra of $E46Q_H$ and $T50V_H$ were therefore considered to be red-shifted as in their dark state.

It has been reported that the PYP mutants in which the hydrogen bond between the chromophore and nearby amino acid was altered have the structures comparable to that of wild type (*35*). On the other hand, the conformational change up to the formation of $PYP_L$ is considered to be small (*32*, *33*). Thus, it is reasonable to speculate that the shape of chromophore binding pocket of the early intermediates of PYP mutant is comparable to that of wild type and that the difference in absorption spectra is attributable to the changes in the interaction between the chromophore and nearby amino acid residues. Because the absorption maximum of *p*-coumaric acid thioester in deprotonated form is about 400 nm (*38*), nearby amino acid residues are responsible for the red shifts of the absorption spectra of $PYP_B$ and $PYP_H$ as well as that of PYP. The mutation of the amino acid residue which interacts with the chromophore causes the shift of absorption spectrum (*9*, *10*). In fact, the absorption maxima of E46Q and T50V are 13 and 8 nm red-shifted from that of the wild type, respectively. Therefore, the red shifts in the absorption spectra of $E46Q_H$, $E46Q_B$, $T50V_H$, and $T50V_B$ show that the chromophores of $PYP_B$ and $PYP_H$ also interact with Glu46 and Thr50. It should be noted that the extents of red shifts in $E46Q_H$ and $E46Q_B$ were larger than those of $T50V_H$, and $T50V_B$. This trend was the same as that in the dark state, and thus, the hydrogen-bonding network is not altered upon formation of the primary intermediates.

Although structural analysis at liquid-nitrogen temperature has not been reported, the structure of $PYP_{BL}$ trapped at −124 °C was previously analyzed by crystallography (*15*). $PYP_{BL}$ is a blue-shifted intermediate thermally formed from $PYP_B$ (*29*). This model shows that the thioester part is flipped in $PYP_{BL}$, and the hydrogen-bonding network around the phenolic oxygen of the chromophore (O4) is maintained. The distances from O4 to O$\eta$ of Tyr42 and O$\epsilon$ of Glu46 are 2.49 and 2.61 Å for the dark state and 2.46 and 2.77 Å for $PYP_{BL}$, respectively, suggesting that the relation of these three oxygen atoms is not altered in $PYP_{BL}$. Our spectroscopic data agree with this model.

*Spectral Analysis of L Intermediates at Low Temperature.* Wild-type PYP in 66% glycerol buffer was cooled to 193 K and irradiated with 436 nm light to trap $PYP_L$ (Figure 4). Upon irradiation of PYP (Figure 4a), the absorbance at 350−460 nm decreased and that at 460−510 nm increased with a clear isosbestic point at 462 nm. The spectral changes before and after the irradiation are calculated by subtracting curve 1 from curves 2−6 and shown in the inset in Figure 4a. E46Q (Figure 4b), T50V (Figure 4c), and R52Q (Figure 4d) were

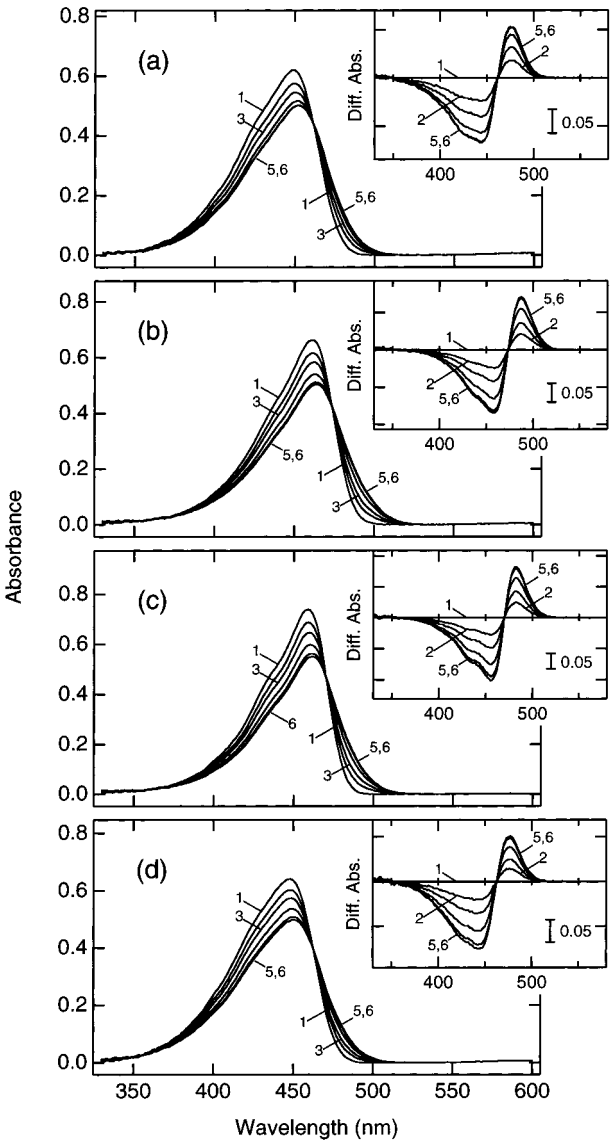


FIGURE 4: Photoreaction of PYP and mutants at 193 K. Wild-type PYP (a), E46Q (b), T50V (c), or R52Q (d) in 66% glycerol buffer was cooled to 193 K (curve 1) and irradiated with 436 nm light for a total of 5, 10, 20, 40, and 80 s (curves 2−6, respectively). Insets: Difference absorption spectra before and after the irradiation were calculated by subtracting curve 1 from curves 2−6 in each data set.

similarly irradiated with 436 nm light, and the difference absorption spectra before and after the irradiation were calculated (insets). They were qualitatively similar to that of wild type, indicating the formation of the intermediates corresponding to $PYP_L$. Curves 6 in the insets of Figure 4a−d were reproduced in Figure 5 after normalization for comparison of the spectra of $PYP_L$, $E46Q_L$, $T50V_L$, and $R52Q_L$. At 193 K, the region of wavelength at which the absorbance of the dark state is small enough (less than 5% of maximal absorbance) is >482 nm for wild type, >490 nm for E46Q, >485 nm for T50V, and >480 nm for R52Q (Figure 4). Because the shapes of positive bands in wild type and R52Q were identical, the absorption spectra of their L intermediates are considered to be identical. However, the difference absorption maxima in E46Q and T50V were 12 and 7 nm red-shifted, respectively. As discussed in the previous section, this finding shows that the interaction among the chromophore, Glu46, and Thr50 in $PYP_L$ is essentially similar to that in the dark state.

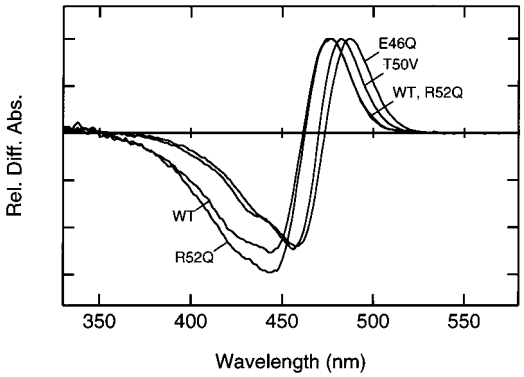


FIGURE 5: Comparison of the absorption spectra of $PYP_L$. Curves 6 in the insets of Figures 4a−d were reproduced after normalization at their difference absorption maxima.

The structure of pR has been analyzed by time-resolved crystallography on a nanosecond time scale (*14*). As mentioned, the difference absorption spectrum between PYP and $PYP_L$ measured at 193 K (*29*) is identical to that at room temperature (*23*, *24*). Therefore, pR and $PYP_L$ are the same species and the spectral similarity indicates that the structure around the chromophore is not changed by cooling. In the model proposed for pR by crystallography, the phenol part is rotated on isomerization. Although the movement of the phenol ring is small, the direction is altered. As a result, O4 of the chromophore no longer faces Glu46 to break the hydrogen bond and approaches Arg52. In contrast, recent FTIR studies for $PYP_L$ at low temperature (*16*) and room temperature (*32*, *33*) strongly suggested that the hydrogen bond between chromophore and Glu46 is maintained in $PYP_L$. The latter model agrees with our present result that the hydrogen-bonding network in $PYP_L$ is similar to that in PYP, $PYP_B$ and $PYP_H$.

*Spectral Analysis of M Intermediates by Flash Photolysis on a Millisecond Time Scale.* Because $PYP_M$ was not trapped at low temperature using 66% glycerol sample (*29*, *37*), it was analyzed by a flash photolysis experiment at room temperature using the sample without glycerol. PYP (Figure 6a), E46Q (Figure 6b), T50V (Figure 6c), and R52Q (Figure 6d) were excited by a yellow flash, and the transient difference absorption spectra before and after excitation were recorded using a multichannel CCD spectroscopy system.

In all samples, absorbance decreases at 380−500 nm and increases at 290−380 nm were observed after excitation. The dark states then recovered as time elapsed. The absorbance changes against time could be fitted by single-order kinetics (data not shown), indicating that only M intermediates were present in this time scale in these samples. The time constants of the decay of $PYP_M$, $E46Q_M$, $T50V_M$, and $R52Q_M$ were 0.24, 0.053, 1.8, and 1.3 s, respectively.

The absorption spectra of M intermediates were calculated from the transient spectra. Namely, the negative bands of curves 1 in Figures 6a−d were canceled by adding the absorption spectra of the respective pigments in the dark states. They are shown in Figure 7 after normalization based on the extinction coefficients of the dark states (*11*). The absorption maxima of $PYP_M$, $E46Q_M$, $T50V_M$, and $R52Q_M$ were located at 357, 368, 357, and 358 nm, respectively. The fact that the absorption maximum of $E46Q_M$ was 11

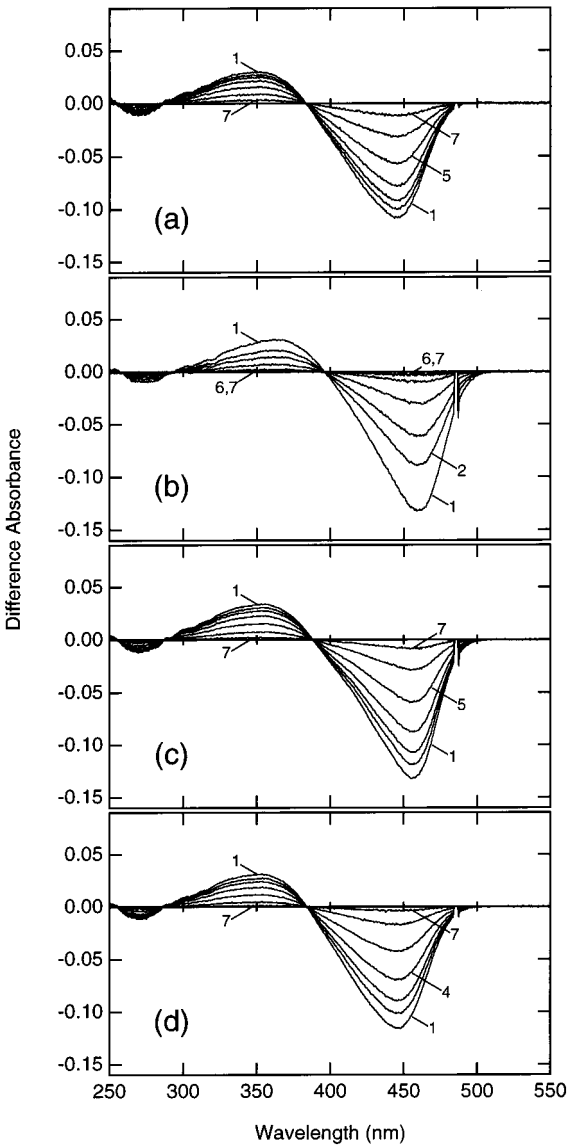


FIGURE 6: Transient difference absorption spectra of wild-type PYP (a), E46Q (b), T50V (c), and R52Q (d) at room temperature. The spectra were recorded at 2, 20, 40, 80, 160, 320, and 640 ms (a and b) or 2, 170, 340, 680, 1360, 2720, and 5440 ms (c and d) after excitation with yellow flash (>410 nm) (curves 1−7, respectively).

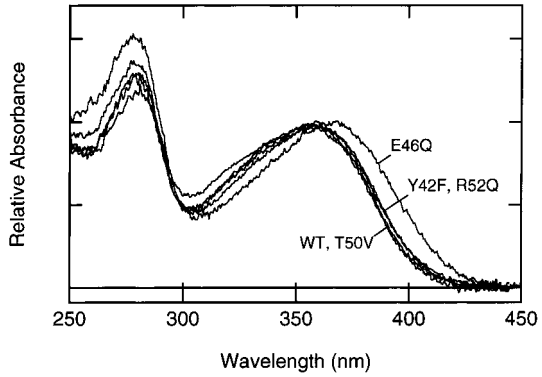


FIGURE 7: Calculated absorption spectra of $PYP_M$, $Y42F_M$, $E46Q_M$, $T50V_M$, and $R52Q_M$.

nm red-shifted shows that the chromophore/protein interaction in the M intermediate is altered by replacement of Glu46 by Gln. In contrast, the absence of a difference in the absorption spectra between $PYP_M$ and $T50V_M$ shows that the interaction between the chromophore and Thr50 is lost in M intermediate.

The interaction between the chromophore and Thr50 is mediated by Tyr42. To clarify whether the interaction between chromophore and Tyr42 is altered in M intermediate, the absorption spectrum of $Y42F_M$ was calculated. We have previously measured the transient spectra for Y42F at room temperature (*11*). Y42F is in the equilibrium between yellow and colorless form at pH 7.0, but the interconversion is much faster than the decay of $Y42F_M$ (*11*). Therefore, even if only the yellow form was excited with >450 nm flash, the repopulation takes place immediately. As a result, the negative band of transient spectra having the spectral shoulder can be canceled well by adding the spectrum of dark state. The absorption spectrum of $Y42F_M$ thus calculated is shown in Figure 7. It is identical to that of $PYP_M$.

The present data demonstrate that Glu46 is involved in the spectral tuning of $PYP_M$, but Tyr42, Thr50, and Arg52 are not. The most straightforward explanation for the red shift of the absorption spectrum of $E46Q_M$ would be that $PYP_M$ retains the hydrogen bond between the chromophore and Glu46. On formation of $PYP_M$, the proton at Glu46 is transferred to the chromophore. The −OH group of the chromophore is hydrogen-bonded with $-COO^-$ group of Glu46, which would be replaced by $-CONH_2$ group of Gln46, resulting in the red shift of the absorption spectrum. This interpretation is based on the assumption that the shape of chromophore binding pocket of $E46Q_M$ is comparable to that of $PYP_M$. Alternatively the amino acid residues near the chromophore would be rearranged by the local or global protein conformational change induced by the mutation, resulting in the different chromophore/protein interaction in $E46Q_M$. FTIR spectroscopy demonstrated that the absorbance change in amide band upon the conversion from E46Q to $E46Q_M$ is smaller than that from PYP to $PYP_M$ (*33*). This may suggest the conformational difference between $PYP_M$ and $E46Q_M$. However, the amide bonds which are responsible for this change in amide mode have not been identified.

The absorption spectrum of $PYP_M$ is not readily changed: it is identical to those of M intermediates from Y42F, T50V, R52Q (this work), and PYPs which lack N-terminal several amino acids (*39*). Therefore, the shape of the chromophore binding pocket in $PYP_M$ is unlikely to be changed by mutation. However, because the experimental evidence to examine the similarity in shapes of chromophore binding pockets of $PYP_M$ and $E46Q_M$ is not sufficient, both possibilities should be taken into consideration.

The structure of $PYP_M$ has previously been analyzed by time-resolved crystallography on a millisecond time scale (*13*) and was the first example of a structure of a PYP intermediate to be determined at high resolution. The model shows that the phenol part of the chromophore rotates on photoisomerization and the movement of this part is much larger than that in the model for $PYP_L$ (*14*). As a results, the hydrogen-bonding network among O4 of the chromophore, O$\eta$ of Tyr42 and O$\epsilon$ of Glu46 is broken and a new hydrogen bond is formed between O4 of the chromophore and Arg52. If this model is applicable to the reaction in the solution, the absorption spectrum of $PYP_M$ would be similar not to $R52Q_M$ but to $E46Q_M$.

In the dark state PYP, Arg52 is located near the chromophore, but it is not as close to the chromophore as Tyr42 and Glu46. The guanidinium group of Arg52 is not close enough to O4 of the chromophore to form a hydrogen bond. The mutational analyses reported so far demonstrated that the replacements of the amino acid residues which are involved in the hydrogen-bonding network around the chromophore induce the spectral shift. However, the amino acid residue which forms no hydrogen bond with the chromophore is not responsible for the spectral tuning even if it is close to the chromophore (for example P68A or Y98F, unpublished result), suggesting that the hydrogen bond between the chromophore and Arg52 is not present in $PYP_M$. Another explanation would be that the chromophore of $PYP_M$ is hydrogen-bonded with Arg52 but it is replaced by the free moving cations in the solution in $R52Q_M$, resulting in no spectral change. However, this cannot explain the absorption spectrum of $PYP_M$ (357 nm), which is different from that in the denatured state (340 nm). If free-moving cations can play the equivalent role to the guanidinium group of Arg52, the absorption maximum of $PYP_M$ would be close to that in the denature state, in which the chromophore is completely exposed to the solvent. Therefore, the former interpretation seems to be likely.

*Model of the PYP Photocycle.* The analysis based on the UV−visible absorption spectra demonstrated that the hydrogen-bonding network around the chromophore is conserved up to $PYP_L$, but it is rearranged upon the formation of $PYP_M$. We recently applied FTIR spectroscopy for analysis of photocycle of PYP (*16*). The results demonstrated that Glu46 is protonated in PYP, $PYP_B$, $PYP_H$, and $PYP_L$ and that it is deprotonated in $PYP_M$. The C═O stretching mode of Glu46 in PYP was located at 1740 $cm^{-1}$, but those of $PYP_B$, $PYP_H$, and $PYP_L$ were located at 1732−1733 $cm^{-1}$. Because the present UV−visible spectroscopy has suggested that Glu46 interacts with the chromophore in $PYP_B$, $PYP_H$, and $PYP_L$, it is reasonable to speculate that the partner of the hydrogen bond of Glu46 is O4 of the chromophore. Therefore, the downshift in C═O stretching mode suggests that the hydrogen bond between chromophore and Glu46 in the intermediate is stronger than that in the dark state. The fact that the wavenumber values for C═O stretching modes of $PYP_B$, $PYP_H$, and $PYP_L$ were constant further indicates that the environment of the hydrogen bond is not altered in these intermediates. The possible model based on our data is shown in Figure 8. The chromophore of PYP in the dark is in a deprotonated trans form, and Glu46 is protonated. On photon absorption, the photocycle of PYP starts with the isomerization of the chromophore. Because it is considered that no large change of the hydrogen-bonding network takes place in $PYP_B$ and $PYP_H$, the ester part of the chromophore would be flipped like the previous model proposed by crystallography of $PYP_{BL}$ (*15*). $PYP_B$ and $PYP_H$ have the chromophores in twisted and deprotonated cis forms, and Glu46 is still protonated. Both of them are relaxed to $PYP_L$. On this conversion process, because the hydrogen bond of Glu46 is not altered as shown by the constant frequency of C═O stretching mode, only a small structural alternation around the phenol part and Glu46 takes place. In contrast, remarkable difference in the vibrational mode of ethylene bond is observed among these intermediates (*16*). Therefore, the distortion of the chromophore at the ethylene bond would

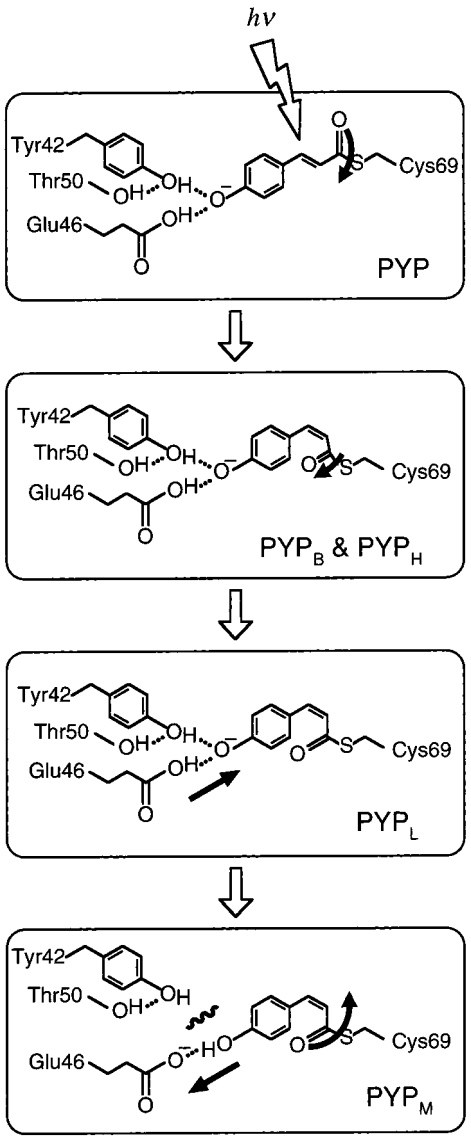


FIGURE 8: Model for the structural changes of the chromophore based on the spectroscopic evidence.

be relaxed by rotating the ester part. $PYP_L$ then converts to $PYP_M$ with proton transfer from Glu46 to the chromophore, which is considered to be the principal cause of the large blue shift. Assuming that the structure of chromophore binding pocket of $PYP_M$ is comparable to that of $E46Q_M$, the red shift of the absorption spectrum of $E46Q_M$ strongly suggests that the hydrogen bond of chromophore with Glu46 is maintained but that with Tyr42 is broken in $PYP_M$, resulting in the global conformational change (*22*).

Our spectroscopic evidence supports the structural model of $PYP_{BL}$ derived from crystallography and that of $PYP_L$ from FTIR. However, there are inconsistencies with the models for $PYP_L$ and $PYP_M$ from crystallography. One possible explanation is that the reaction pathway in the crystal is not necessarily the same as that in the solution. The combination of spectroscopic technique and crystallography is expected to reveal the nature of the photoreaction of PYP.

## REFERENCES

1. Meyer, T. E. (1985) *Biochim. Biophys. Acta 806*, 175−183.
2. Sprenger, W. W., Hoff, W. D., Armitage, J. P., and Hellingwerf, K. J. (1993) *J. Bacteriol. 175*, 3096−3104.

3. Baca, M., Borgstahl, G. E. O., Boissinot, M., Burke, P. M., Williams, D. R., Slater, K. A., and Getzoff, E. D. (1994) *Biochemistry 33*, 14369−14377.
4. Borgstahl, G. E. O., Williams, D. R., and Getzoff, E. D. (1995) *Biochemistry 34*, 6278−6287.
5. Düx, P., Rubinstenn, G., Vuister, G. W., Boelens, R., Mulder, F. A., Hård, K., Hoff, W. D., Kroon, A. R., Crielaard, W., Hellingwerf, K. J., and Kaptein, R. (1998) *Biochemistry 37*, 12689−12699.
6. Van Beeumen, J. J., Devreese, B. V., Van Bun, S. M., Hoff, W. D., Hellingwerf, K. J., Meyer, T. E., McRee, D. E., and Cusanovich, M. A. (1993) *Protein Sci. 2*, 1114−1125.
7. Hoff, W. D., Düx, P., Hård, K., Devreese, B., Nugteren-Roodzant, I. M., Crielaard, W., Boelens, R., Kaptein, R., Van Beeumen, J., and Hellingwerf, K. J. (1994) *Biochemistry 33*, 13959−13962.
8. Imamoto, Y., Ito, T., Kataoka, M., and Tokunaga, F. (1995) *FEBS Lett. 374*, 157−160.
9. Mihara, K., Hisatomi, O., Imamoto, Y., Kataoka, M., and Tokunaga, F. (1997) *J. Biochem. (Tokyo) 121*, 876−880.
10. Genick, U. K., Devanathan, S., Meyer, T. E., Canestrelli, I. L., Williams, E., Cusanovich, M. A., Tollin, G., and Getzoff, E. D. (1997) *Biochemistry 36*, 8−14.
11. Imamoto, Y., Koshimizu, H., Mihara, K., Hisatomi, O., Mizukami, T., Tsujimoto, K., Kataoka, M., and Fumio Tokunaga (2001) *Biochemistry 40*, 6047−6052.
12. Kort, R., Vonk, H., Xu, X., Hoff, W. D., Crielaard, W., and Hellingwerf, K. J. (1996) *FEBS Lett. 382*, 73−78.
13. Genick, U. K., Borgstahl, G. E., Ng, K., Ren, Z., Pradervand, C., Burke, P. M., Srajer, V., Teng, T. Y., Schildkamp, W., McRee, D. E., Moffat, K., and Getzoff, E. D. (1997) *Science 275*, 1471−1475.
14. Perman, B., Šrajer, V., Ren, Z., Teng, T., Pradervand, C., Ursby, T., Bourgeois, D., Schotte, F., Wulff, M., Kort, R., Hellingwerf, K., and Moffat, K. (1998) *Science 279*, 1946−1950.
15. Genick, U. K., Soltis, S. M., Kuhn, P., Canestrelli, I. L., and Getzoff, E. D. (1998) *Nature 392*, 206−209.
16. Imamoto, Y., Shirahige, Y., Tokunaga, F., Kinoshita, T., Yoshihara, K., and Kataoka, M. (2001) *Biochemistry 40*, 8997−9004.
17. Xie, A., Hoff., W. D., Kroon, A. R., and Hellingwerf, K. J. (1996) *Biochemistry 35*, 14671−14678.
18. Imamoto, Y., Mihara, K., Hisatomi, O., Kataoka, M., Tokunaga, F., Bojkova, N., and Yoshihara, K. (1997) *J. Biol. Chem. 272*, 12905−12908.
19. van Brederode, M. E., Gensch, T., Hoff, W. D., Hellingwerf, K. J., and Braslavsky, S. E. (1995) *Biophys. J. 68*, 1101−1109.
20. Rubinstenn, G., Vuister, G. W., Mulder, F. A., Düx, P. E., Boelens, R., Hellingwerf, K. J., and Kaptein, R. (1998) *Nat. Struct. Biol. 5*, 568−570.
21. Hoff, W. D., Xie, A., Van Stokkum, I. H., Tang, X. J., Gural, J., Kroon, A. R., and Hellingwerf, K. J. (1999) *Biochemistry 38*, 1009−1017.
22. Ohishi, S., Shimizu, N., Mihara, K., Imamoto, Y., and Kataoka, M. (2001) *Biochemistry 40*, 2854−2859.
23. Meyer, T. E., Yakali, E., Cusanovich, M. A., and Tollin, G. (1987) *Biochemistry 26*, 418−423.
24. Hoff, W. D., Van Stokkum, I. H. M., Van Ramesdonk, H. J., Van Brederode, M. E., Brouwer, A. M., Fitch, J. C., Meyer, T. E., Van Grondelle, R., and Hellingwerf, K. J. (1994) *Biophys. J. 67*, 1691−1705.
25. Ujj, L., Devanathan, S., Meyer, T. E., Cusanovich, M. A., Tollin, G., and Atkinson, G. H. (1998) *Biophys. J. 75*, 406−412.
26. Devanathan, S., Pacheco, A., Ujj, L., Cusanovich, M., Tollin, G., Lin, S., and Woodbury, N. (1999) *Biophys. J. 77*, 1017−1023.
27. Imamoto, Y., Kataoka, M., Tokunaga, F., Asahi, T., and Masuhara, H. (2001) *Biochemistry 40*, 6047−6052.
28. Hoff, W. D., Kwa, S. L. S., Van Grondelle, R., and Hellingwerf, K. J. (1992) *Photochem. Photobiol. 56*, 529−539.
29. Imamoto, Y., Kataoka, M., and Tokunaga, F. (1996) *Biochemistry 35*, 14047−14053.
30. Shichida, Y., Ono, T., Yoshizawa, T., Matsumoto, H., Asato, A. E., Zingoni, J. P., and Liu, R. S. H. (1987) *Biochemistry 26*, 4422−4428.
31. Borhan, B., Souto, M. L., Imai, H., Shichida, Y., and Nakanishi, K. (2000) *Science 288*, 2209−2212.
32. Brudler, R., Rammelsberg, R., Woo, T. T., and Getzoff, E. D. (2001) *Nat. Struct. Biol. 8*, 265−270.
33. Xie, A., Kelemen, L., Hendriks, J., White, B. J., Hellingwerf, K. J., and Hoff, W. D. (2001) *Biochemistry 40*, 1510−1517.
34. Devanathan, S., Brudler, R., Hessling, B., Woo, T. T., Gerwert, K., Getzoff, E. D., Cusanovich, M. A., and Tollin, G. (1999) *Biochemistry 38*, 13766−13772.
35. Brudler, R., Meyer, T. E., Genick, U. K., Devanathan, S., Woo, T. T., Millar, D. P., Gerwert, K., Cusanovich, M. A., Tollin, G., and Getzoff, E. D. (2000) *Biochemistry 39*, 13478−13486.
36. Devanathan, S., Lin, S., Cusanovich, M. A., Woodbury, N., and Tollin, G. (2000) *Biophys. J. 79*, 2132−2137.
37. Meyer, T. E., Tollin, G., Hazzard, J. H., and Cusanovich, M. A. (1989) *Biophys. J. 56*, 559−564.
38. Kroon, A. R., Hoff, W. D., Fennema, H. P., Gijzen, J., Koomen, G. J., Verhoeven, J. W., Crielaard, W., and Hellingwerf, K. J. (1996) *J. Biol. Chem. 271*, 31949−31956.
39. Harigai, M, Yasuda, S., Imamoto, Y., Yoshihara, K., Tokunaga, F., and Kataoka, M. (2001) *J. Biochem. (Tokyo) 130*, 51−56.


BI010468U